Ortuño Cases, C.; Quiles Chuliá, MD.; Benedito Fort, JJ. (2014). Inactivation kinetics and cell morphology of E.coli and S.carevisiae trated with ultrasound-assited supercritical CO2. Food Research International. 62:955-964. doi:10.1016.

Inactivation kinetics and cell morphology of *E. coli* and *S. cerevisiae* treated with ultrasound-assisted supercritical CO_2

Carmen Ortuño[1], Amparo Quiles[2], Jose Benedito[1]*

[1] Grupo de Análisis y Simulación de Procesos Agroalimentarios, Departamento Tecnología de Alimentos, Universitat Politècnica de València, Camí de Vera s/n, E46022, Valencia, Spain.

[2] Grupo de Microestructura y Química de Alimentos, Departamento Tecnología de Alimentos, Universitat Politècnica de València, Camí de Vera s/n, E46022, Valencia, Spain.

*Corresponding author: Grupo de Análisis y Simulación de Procesos Agroalimentarios, Departamento Tecnología de Alimentos, Universitat Politècnica de València, Camí de Vera s/n, E46022, Valencia, Spain. Tel.: +34-96-3879147 Fax: +34-96-3879839.

E-mail address: jjbenedi@tal.upv.es (Jose Benedito)

ABSTRACT

The inactivation kinetics of *Escherichia coli* (*E. coli*) and *Saccharomyces cerevisiae* (*S. cerevisiae*) cells in apple juice subjected to supercritical carbon dioxide (SC-CO_2) assisted by high power ultrasound (HPU) at different pressures (100-350 bar, 36 ºC) and temperatures (31-41 ºC, 225 bar) were studied. On average, shorter process times were required to achieve the total inactivation of *S. cerevisiae* (2-6 min) in apple juice than *E. coli* (7 min). The inactivation kinetics of *E. coli* and *S. cerevisiae* were satisfactorily described by the Peleg Type A and the Weibull model, respectively, considering temperature and pressure as model parameters. Transmission electron microscopy (TEM) and light microscopy (LM) techniques were used to study the cellular changes of SC-CO_2 (350 bar, 36 ºC, 5 min) and SC-CO_2+HPU (350 bar, 36 ºC, 5min, 40 W) treated cells. TEM and LM images revealed that 5 min of SC-CO_2 treatment generated minor morphological modifications, although no inactivation of the cells was obtained. However, 5 min of SC-CO_2+HPU treatment totally inactivated the population of both microorganisms. SC-CO_2+HPU produced the degradation of the internal cell content and the disruption of the cell wall and plasmalemma, which prevented the possible regrowth of the cells during refrigerated storage.

Key words: microbial inactivation, apple juice, transmission electron microscopy, cellular morphology, supercritical carbon dioxide, high power ultrasound.

1. INTRODUCTION

The current market share of apple juice is rising, since it is perceived as "healthy" food due to its high content in polyphenols and flavonoids, which contribute to its good antioxidant properties (Kumar, Thippareddi, Subbiah, Zivanovic, Davinson, & Harte, 2009). However, apple juice is commonly spoiled by the presence and growth of its natural acid tolerant and osmophilic microflora (Tahiri, Makhlouf, Paquin, & Fliss, 2006) and can be a vehicle for external spoilage microorganisms and pathogens.

The preservation technologies developed during the last few years, have been driven by the relentless pursuit to reduce the degree of thermal damage to the quality of thermally processed foods (Rawson, Patras, Tiwari, Noci, Koutchma, Brunton, 2011). In order to obtain safe products with fresh-like quality attributes, a novel inactivation technique based on High Power Ultrasound (HPU) embedded in a Supercritical Carbon Dioxide (SC-CO_2) System has been developed (Benedito, Martínez-Pastor, Mulet, Ortuño, & Peña, 2011).

The simultaneous application of SC-CO_2 and HPU has been shown to accelerate the death of *Escherichia coli* (*E. coli*) and *Saccharomyces cerevisiae* (*S. cerevisiae*) inoculated in different media. Ortuño, Martínez-Pastor, Mulet, & Benedito (2012a, 2013) showed that the population of both microorganisms inoculated in apple juice, was completely inactivated after 5 min (350 bar, 36 ºC) and 4 min (225 bar, 36 ºC) of treatment, respectively. No microbial reduction was observed with only SC-CO_2 under the same conditions. These authors explored the inactivation in juices using a single combination of pressure and temperature. No references have been found in the literature exploring and modeling the effect of temperature and pressure on the inactivation of microorganisms in real foods, such as apple juice, using SC-CO_2+HPU.

The mechanisms of microbial inactivation by SC-CO_2+HPU have not yet been fully elucidated. Combining SC-CO_2 and HPU the solubilization rate of SC-CO_2 into the liquid and the increase in the mass transfer due to the vigorous agitation produced by the ultrasonic field would permit the rapid saturation of CO_2 in the medium, which might accelerate the inactivation mechanisms (a decrease of the medium pH, an increase in membrane fluidity and permeability, the diffusion of CO_2 into the cells, cell membrane rupture, the alteration of intracellular equilibrium, the inactivation of key enzymes, and the extraction of critical intracellular materials) of the SC-CO_2 inactivation treatments (Garcia-Gonzalez et al., 2007). The phenomenon of cavitation could damage the cell walls causing the death of the microbial cells (Ortuño et al., 2012a, 2013).

Different authors pointed out that there is a direct relationship between the cellular modification and the inactivation caused by SC-CO_2 (Garcia-Gonzalez, Geeraerd, Mast, Briers, Elst, Van Ginneken, Van Impe, & Devlieghere, 2010; Liao, Zhang, Liao, Hu, Chen, & Deng, 2010a). Although different studies have been conducted regarding the ultrasound-assisted inactivation of microorganisms using SC-CO_2 (Ortuño et al., 2012a, 2013), no references have been found in literature covering a detailed study of the cellular damage and morphological changes generated by SC-CO_2+HPU treatments in microbial cells.

Therefore, the objective of this work was to study the effect of HPU-assisted SC-CO_2 treatments on the inactivation kinetics of *E. coli* and *S. cerevisiae* cells inoculated in apple juice and to study the cellular damage caused to microorganisms by this novel technology.

2. MATERIAL AND METHODS

2.1. Apple juice

Apples (*Golden delicious*) were purchased from a local market and kept at 4ºC for 2 days until juice extraction. The apples were washed, diced and squeezed using a screw juice extractor (Ultra Juicer, Robot Coupe J80, USA) to obtain the juice. ºBrix was measured in triplicate using a digital refractometer (Hand-held Pocket, ATAGO). The apple juice (pH = 5.4; ºBrix = 15.6) produced was sealed in plastic containers and stored at -18 ºC until required.

2.2. Microorganisms strains and inoculated media

The microbial strains used in this study were *Escherichia coli* DH1 and *Saccharomyces cerevisiae* T73. A single colony of *E. coli* or *S. cerevisiae* was grown overnight in Luria Bertani Broth (LB Broth, Sigma-Aldrich, USA) at 37ºC, or in Yeast Peptone Dextrose Broth (YPD Broth, Sigma- Aldrich, USA) at 30ºC, respectively, using an incubation chamber (J.P. SELECTA, Model 3000957, Barcelona, Spain) and an orbital shaker at 120 rpm (J.P. SELECTA, Rotabit Model 3000974, Barcelona, Spain). For each experiment with *E. coli* or *S. cerevisiae*, a subculture was prepared by inoculating 50 µL from the starter culture into 50 mL sterilized medium and incubating at 37 ºC-24 h or at 30 ºC-24 h, respectively.

For each experiment with juice, a plastic container with 50 mL of apple juice was thawed at 4 ºC for 12 h before processing to evaluate the inactivation kinetics. The inoculated juice was prepared by adding 5 mL of either *E. coli* or *S. cerevisiae* cells to 50 mL of apple juice, to reach a cell concentration of 10^6-10^8 CFU/mL.

To evaluate the individual effect of SC-CO_2 and SC-CO_2+HPU treatments on the cell morphology of *E. coli* and *S. cerevisiae* and the regrowth capacity of these

120 microorganisms (storage test), each sample was prepared by adding 5 mL of either *E.*
121 *coli* or *S. cerevisiae* cells to 50 mL of LB or YPD Broth culture, respectively. The LB
122 and YPD Broths were selected as the treatment media for the ultrastructural analysis for
123 two reasons: they were the simplest media where SC-CO_2+HPU has been applied to
124 inactivate these microorganisms (Ortuño et al., 2012a, 2013), and also to prevent the
125 suspended solids and sugars present in apple juice to affect the analysis of images.

126 2.3. Experimental design

127 In order to evaluate the inactivation kinetics of *S. cerevisiae* and *E. coli*, the
128 inoculated apple juice was subjected to the SC-CO_2+HPU treatment under different
129 pressures (100, 225 and 350 bar, 36 ºC) and temperatures (31, 36 and 41 ºC, 225 bar).
130 The temperatures chosen were higher than the critical one for CO_2 and lower than lethal
131 temperatures for *E. coli* and *S. cerevisiae*. The pressures chosen were higher than the
132 critical one for CO_2 (73.8 bar) and lower than 350 bar according to previous studies
133 where it was observed that pressures higher than 350 bar were not necessary to reach 7-
134 8 log reductions using SC-CO_2+HPU (Ortuño et al., 2012a, 2013).

135 In order to evaluate the effect of SC-CO_2 and SC-CO_2+HPU treatments on the
136 morphological changes and the regrowth capacity of *E. coli* and *S. cerevisiae* treated
137 cells (storage test), the inoculated culture medium was subjected to SC-CO_2 at 350 bar,
138 36 ºC for 5 min or to SC-CO_2+HPU treatments at 350 bar, 36 ºC and 40 ± 5 W, for
139 5 min. These conditions were selected because it has been previously demonstrated
140 (Ortuño et al., 2012a, 2013) that when using SC-CO_2+HPU, temperatures higher than
141 36 ºC, pressures higher than 350 bar, or process times longer than 5 min are not
142 necessary to achieve the total inactivation of these microorganism inoculated in the
143 culture medium.

144 2.4. Supercritical fluid equipment and processing procedure

2.4.1. Apparatus

The experiments were carried out in a batch supercritical fluid lab-scale equipment especially designed and built for this application by the research group (Fig. 1). The system includes ultrasound equipment (Benedito et al., 2011) which is embedded in the supercritical fluids vessel. The ultrasound equipment consists of a high power piezoelectric transducer, an insulation system and a power generator unit (40 W ± 5 W). The transducer is inserted inside the inactivation vessel and includes two commercial ceramics (35 mm external diameter; 12.5 mm internal diameter; 5 mm thickness; resonance frequency of 30 kHz) and a sonotrode, which was specially constructed to concentrate the highest amount of acoustic energy on the application point. The equipment is described in detail by Ortuño et al. (2013).

2.4.2. Supercritical fluid processing

Prior to each experiment, the inactivation vessel was cleaned and sanitized with disinfectant solution, distilled water and autoclaved water. For each experiment, a subculture was prepared by inoculating 5 mL of cells in the early stationary phase (prepared as described in section 2.2) in 50 mL of sterilized apple juice or culture medium to a cell concentration of 10^6-10^7 CFU/mL.

The sample (55 mL), inoculated apple juice or culture medium, was loaded into the inactivation vessel and immediately sealed. The pump filled the vessel with supercritical carbon dioxide, reaching the desired pressure in less than 2.5 min. Time zero for each treatment was taken when the experimental temperature and pressure were reached. For the experiments with HPU, the ultrasound unit was turned on (time zero) when the desired pressure and temperature were reached in the vessel, the applied power during the whole experiment being 40 W ± 5 W (I = 181 mA ± 18 mA; U = 220 V ± 5 V) (Power measured using a Digital Power Meter, Yokogawa, Model WT210).

Pressure and temperature were kept constant during the experiment through the pump and the thermostatic bath, respectively. All the experiments were run in triplicate.

For the inactivation treatments with inoculated apple juice, samples of 1 mL were extracted periodically through a small tube located at the bottom of the inactivation vessel until the end of the experiment. This tube was cleaned and disinfected with 3 mL of ethanol (96 %v/v) after each sampling. The treated samples were collected in individual sterile plastic test tubes for microbial enumeration.

In the inactivation treatments for the morphological study, all the sample volume was extracted and collected after the treatment.

For the storage test, samples containing the treated cells were collected at the end of each treatment, divided in 7 sterile tubes and placed at refrigerated temperature (4 ºC) for 6 weeks. At time 0 (after the treatment), and weekly from the 1st to the 6th week of storage, the viability of the microorganisms was evaluated.

2.5. Enumeration of viable microorganisms

The viability of the non-treated and SC-CO_2+HPU treated cells was assessed via a spread plating method on specific selective agars, LB Agar or YPD Agar and incubated for 24 h at 37 ºC or 30 ºC, for *E. coli* or *S. cerevisiae* respectively, before counting. The results were expressed as log (N/N_0) versus time, where N_0 is the initial number of cells in the control sample and N is the number of cells in the sample after the different times of treatment. The data presented for each treatment condition are the means of the triplicate experiments. Moreover, it was shown for each experiment the arithmetic mean and the standard deviation of log (N/N_0) for at least three plates.

2.6. Mathematical models and fitting of data

According to the results of previous studies which have addressed the modelling of microbial inactivation using SC-CO_2, HPU or SC-CO_2+HPU (Peleg, 2006; Lee et al., 2009; Corradini and Peleg, 2012; Ortuño et al., 2013), four different models (Table 1) have been selected in this study to fit the inactivation kinetics of the selected microorganisms treated with SC-CO_2+HPU in apple juice.

2.7. Transmission electron microscopy (TEM) and Light Microscopy (LM)

The cells treated by SC-CO_2 or SC-CO_2+HPU, were collected at the end of the treatment and centrifuged at 2600 rpm and 4ºC for 5 min. The pellets were collected and fixed with 25 g/L glutaraldehyde solution for 24 h at 4ºC and post-fixed with 20 g/L osmium tetroxide solution for 1.5 h. The cells were centrifuged and the pellet collected. This procedure was applied after each step of the process.

After this process, cells were stabilized by mixing them with a low gelling temperature agarose solution (3 g/100 mL) at 30 ºC, which facilitates fixation and embedding prior to LM and TEM observation. Hereafter, the cells inserted in the solidified agar were cut into cubes (1 mm^3). These cubes were fixed with 25 g/L glutaldehyde solution; post-fixed with 20 g/L osmium tetroxide solution; dehydrated with 30 g/L, 50 g/L, 70 g/L ethanol and 100 g/L; contrasted with uranyl acetate solution (20 g/L) and embedded in epoxy resin (Durcupan, Sigma–Aldrich, St. Louis, MO, USA). The blocks obtained were cut using a Reichter-Jung ULTRACUT ultramicrotome (Leica Mycrosystems, Wetzlar, Germany). Semithin sections (1.5 µ) were stained with 1 g/L toluidine blue and examined in a Nikon Eclipse E800 light microscope (Nikon, Tokyo, Japan). The ultrathin sections obtained (0.1 µm) were collected in copper grids and stained with 20 g/L acetate uranile and 40 g/L lead citrate to be observed in the Philips EM 400 Transmission Electron Microscope (Eindhoven, Holland) at 80 kV.

2.8. Image analysis

The image analysis was carried out using the software ImageJ (Rasband, W.S., ImageJ v. 1.43 s, National Institute of Health, Bethesda, MD, USA). The dimension of cells and the thickness of the cell walls were determined using TEM images. All the measurements were assessed from at least twelve randomly acquired TEM images.

2.9. Statistical analysis

The statistics package Statgraphics Plus (Statistical Graphics Corp. 5.1, Warrenton, USA) was used to perform a simple ANOVA to determine the effect of the treatments on the dimensions of both microorganisms. Moreover, multifactorial ANOVA, and LSD (Least Significant Differences) were used to evaluate the effect of pressure, temperature and time on the inactivation rate of microorganisms.

The kinetic constants of the models were calculated by minimizing the sum of the square differences between experimental and model-predicted data using the Solver Microsoft Excel^{TM} tool. The root mean square error (RMSE) and the coefficient of determination (R^2) were used to evaluate the model's goodness of fit and the estimation accuracy (Schemper, 2003).

3. RESULTS AND DISCUSSION

3.1. SC-CO_2+HPU inactivation of *E. coli* cells. Kinetics and modeling.

The inactivation curves of *E. coli* cells in apple juice undergoing a combined SC-CO_2+HPU process at different temperatures (Fig. 2A) and pressures (Fig. 2B) represented a fast-to-slow curve. No shoulders were observed for any temperature and pressure condition studied and the viability began to decrease quickly, starting to slow down after 1 min. Reductions of 4.6, 5.1 and 5.6 log-cycles were obtained after 1 min of

242 treatment at 225 bar and 31, 36 and 41 ºC, respectively; and reductions of 3.3, 5.1 and
243 4.2 log-cycles were obtained after 1 min of treatment at 36 ºC and 100, 225 and 350 bar,
244 respectively. After the first minute, the population decreased slowly and on average, a
245 reduction of 7.5 log-cycles was obtained after 7 min of treatment under every condition
246 studied. No significant differences ($p>0.05$) were found either between the temperatures
247 or the pressure conditions selected; therefore, the effect of increasing the temperature or
248 pressure did not significantly increase the inactivation level of *E. coli* inoculated in
249 apple juice.

250 The inactivation of *E. coli* has been explored in previous studies using SC-CO_2.
251 Liao, Hu, Liao, Chen, & Wu (2006) studied the inactivation of *E. coli* with a batch SC-
252 CO_2 system in cloudy apple juice and found that the inactivation level rose as the
253 temperature and pressure increased: from 5 to 7 log-cycles by increasing the
254 temperature from 32 to 42 ºC (300 bar, 75 min); and from 5.5 to 7.5 log-cycles by
255 increasing the pressure from 100 to 300 bar (42 ºC, 75 min), respectively. Shimoda,
256 Yamamoto, Cocunubo-Castellanos, Tonoike, Kawano, Ishikawa, & Osajima (1998)
257 studied the antimicrobial effects of pressurized carbon dioxide in a continuous flow
258 system on the population of *E. coli* (10^8-10^9 CFU/mL), inoculated in phosphate buffer.
259 No survivors were found after 15 min of residence time under 35 ºC and 60 bar. This
260 fact could be due to a better agitation in continuous systems that might enhance mass
261 transfer and solubilization rates of pressurized CO_2 in the liquid phase, and increase the
262 contact of CO_2 with microbial cells (Erkmen, 2012). Compared to the results of this
263 work, in the studies where batch systems were used, the inactivation rate increased as
264 the temperature and pressure rose, but much longer process times were needed
265 compared to SC-CO_2+HPU processing. Moreover, the HPU-assisted batch supercritical

266 system of the present study allowed similar inactivation levels to be attained in shorter
267 process times than when using continuous SC-CO_2 systems.

268 The process time needed in the present study to attain the total inactivation of *E.*
269 *coli* inoculated in apple juice was 7 min, which was longer compared to the 2-3 min
270 required with LB Broth (Ortuño el at., 2012a). The inactivation rate of the
271 microorganisms treated with SC-CO_2 is seriously affected by the constituents of the
272 suspending media and/or the nature of the treated foods (Garcia-Gonzalez, Geeraerd,
273 Spilimbergo, Elst, Van Ginneken, Debevere, Van Impe, & Devlieghere, 2007). The
274 sugars of the apple juice (15.6 ºBrix, approximately 93.5 % higher than in LB Broth),
275 bind water from the medium and the amount of free water in which CO_2 could be
276 dissolved is lower than in LB Broth (Ferrentino, Balaban, Ferrari, & Poletto, 2010)
277 despite the intense ultrasound agitation. The effect of higher sugar content of apple juice
278 limited the effect of increasing the pressure or temperature and could not facilitate the
279 solubilization of CO_2 into the medium (Liao et al., 2006) and the subsequent
280 inactivation mechanisms. Therefore, it has been shown that the nature of the medium
281 drastically influences the effect of SC-CO_2+HPU on *E. coli*.

282 Additionally, the inactivation kinetics of *E. coli* treated with SC-CO_2 and HPU
283 were fitted by using the four models described in Table 1. Table 2 shows the statistical
284 parameters for the fit of the kinetic models to the inactivation data of *E. coli* in apple
285 juice. R^2 and RMSE values (Table 2) indicate that, overall, a good fit was obtained with
286 the four models under the different process conditions considered. $R^2 > 0.94$ were found
287 for most of the conditions studied except using the Biphasic model (R^2_{avg} = 0.86;
288 $RMSE_{avg}$ = 0.591). On average, the Peleg Type A model (R^2_{avg} = 0.961; $RMSE_{avg}$ =
289 0.386) provided the best fit for all the process conditions selected, therefore it was

selected in order to predict the inactivation kinetics of *E. coli* at any pressure and temperature in the range of the variables considered.

Since the pressure and temperature were not significant factors ($p>0.01$) in the inactivation of *E. coli*, the inactivation kinetics obtained at different pressures and temperatures were fitted to the same equation using the Peleg Type A model. The parameters, a_1, a_2, and a_3, were calculated by minimizing the sum of square differences between all the experimental data and all the predicted data considered for every pressure and temperature condition studied. The values of the a_1, a_2, and a_3 parameters were 6.38, -0.02 min^{-1} and -0.56 min, respectively. A general expression of the Peleg Type A model was obtained that could be used to predict the inactivation kinetics of *E. coli* in apple juice for any pressure and temperature in the studied range (Fig. 2). The statistical parameters of the general Peleg Type A model exhibited a worse fit of the *E. coli* inactivation kinetics (R^2_{avg} = 0.936 and $RMSE_{avg}$ = 0.561) compared to the average of the individual fits to each survival curve obtained at each temperature and pressure (R^2_{avg} = 0.961; $RMSE_{avg}$ = 0.386). However, according to the R^2 and RMSE values, could be concluded that the proposed general model properly described the SC-CO_2+HPU inactivation kinetics of *E. coli* in apple juice, for any condition of pressure and temperature in the selected range, 100-350 bar and 31-41 ºC, respectively.

3.2. SC-CO_2+HPU inactivation of *S. cerevisiae* cells. Kinetics and modeling.

In the inactivation kinetics of *S. cerevisiae*, no lag phase was observed for any condition studied and the viability began to decrease immediately. Fig. 3A showed a fast-to-slow kinetic for all the temperatures studied. The population reductions obtained after 1 min of treatment were 1.8, 3.9 and 4.8 log-cycles, at 31, 36 and 41 ºC, respectively. Total reduction was reached after 4 and 2 min at 36 and 41 ºC, respectively, but only 3.4 log-cycles reduction was attained after 6 min at 31 ºC. On

315 average, the inactivation rate increased significantly ($p<0.05$) as the temperature rose
316 from 31 ºC to 36 ºC and from 36 ºC to 41 ºC.

317 Reductions of 2.9 and 3.9 log-cycles were obtained after 1 min of treatment, at 100
318 and 225 bar, respectively (Figure 3B). The inactivation kinetics at 100 and 225 bar
319 behaved in a similar way and, on average, no significant differences ($p>0.05$) were
320 found between them. However, when the pressure was increased to 350 bar, a
321 significantly ($p<0.05$) faster inactivation was observed than at 100 and 225 bar. At 350
322 bar, total inactivation was attained after only 1 min of treatment. Therefore, the effect of
323 increasing temperature or pressure, significantly accelerated the inactivation of *S.*
324 *cerevisiae* in apple juice, although pressures of over 225 bar were necessary to observe
325 a significant pressure effect.

326 The inactivation of *S. cerevisiae* with SC-CO_2 has been explored by other authors.
327 Erkmen (2003) reduced the microbial population of *S. cerevisiae* inoculated in potato
328 dextroxe broth with a batch SC-CO_2 system. The time needed to attain total reduction
329 fell from 165 to 50 min and from 125 to 65 min as the temperature increased from 30 to
330 50 ºC at 75 and 100 bar, respectively. Spilimbergo, Mantoan, & Dalser (2007) used a
331 multi-batch system to study the SC-CO_2 pasteurization of apple juice inoculated with *S.*
332 *cerevisiae*. The microbial reduction increased from 3.9 to 4.5 logs when the pressure
333 rose from 100 to 200 bar, after 30 min of process. In the aforementioned works, an
334 increase in the inactivation level was also generally observed as the pressure and
335 temperature rose, although they required much longer times than when using SC-
336 CO_2+HPU.

337 Contrary to the results observed in previous studies using SC-CO_2+HPU to
338 inactivate *S. cerevisiae* in YPD Broth medium (Ortuño et al., 2013), where the effect of
339 increasing the pressure and temperature did not increase the inactivation rate, in the

present study with apple juice, the inactivation rate increased with pressure and temperature. As previously explained, the inactivation rate is affected by the composition of the suspending medium (Garcia-Gonzalez et al., 2007; Ortuño et al., 2013). The high sugar content of apple juice could limit the fast CO_2 saturation of the apple juice in spite of the intense ultrasound agitation. As a consequence, an increase in pressure increases the theoretical solubility of CO_2 which raises the level of dissolved CO_2 into the apple juice; and temperature may have a viscosity effect on the dissolved CO_2 by speeding up mass transfer.

On average, *E. coli* showed more resistance to SC-CO_2+HPU treatments than *S. cerevisiae*, in contrast to the results obtained in previous studies (Ortuño, Martínez-Pastor, Mulet, & Benedito, 2012b). In treatments with apple juice, where despite the effect of HPU the high sugar content could limit the fast solubilization of CO_2 into the medium, it could be thought that the inactivation mechanism would be greatly affected by the cavitation phenomenon and the size of the microorganism. The size of *S. cerevisiae* cells, 8-10 µm (Laun, Pichova, Madeo, Fuchs, Ellinger, Kohlwein, Dawes, Fröhlich, & Breitenbach, 2001), is much larger than *E. coli* cells, 1.2-2 µm (Nelson, & Young, 2000); therefore, the likelihood that the implosion of the cavitation bubbles might reach and affect the cell structure could be higher for *S. cerevisiae* than for *E. coli*. Thus, HPU had a different effect on the SC-CO_2 inactivation of different microorganisms inoculated in apple juice.

Similarly to *E. coli*, the inactivation kinetics of *S. cerevisiae* cells in apple juice subjected to SC-CO_2+HPU were fitted using the models described in Table 1. The statistical parameters obtained from the fit of the experimental data are shown in Table 2. The four models satisfactorily described the inactivation kinetics of *S. cerevisiae* ($R^2 > 0.96$), and on average the Weibull model ($R^2_{avg} = 0.986$; $RMSE_{avg} =$

365 0.198) provided the best fit for all the process conditions selected. The Weibull model
366 was selected in order to predict the inactivation of *S. cerevisiae* at any pressure and
367 temperature in the range of the variables considered in this study.

368 From the ANOVA of *S. cerevisiae* inactivation kinetics, both pressure and
369 temperature were found to be significant factors ($p<0.01$); so we assumed that the
370 parameters of the Weibull model, b and n, could be described by a log-logistic model
371 (Peleg 2006), with simultaneous pressure and temperature dependence (Eqs. (3, 4)).

372 $$b(T,P) = \ln(1+\exp(x_b(T-T_c)+z_b(P-P_c)) \quad \text{Eq. (3)}$$

373 $$n(T,P) = \ln(1+\exp(x_n(T-T_c)+z_n(P-P_c)) \quad \text{Eq. (4)}$$

374 where x_b, z_b, x_n, z_n, T_c and P_c are the characteristic constants of the microorganism.
375 Substituting Eqs. (3, 4) in the Weibull model (Table 1), a general expression of the
376 model was obtained that could be used to predict the inactivation kinetics of
377 *S. cerevisiae* in apple juice for different pressures and temperatures (Fig. 3).

378 The values of the characteristic constants for this general model were calculated by
379 minimizing the sum of square differences between all the experimental data and all the
380 data predicted by the model considering every pressure and temperature condition
381 studied. The values of the coefficients x_b, z_b, x_n, z_n, T_c and P_c were 0.373 $^oC^{-1}$,
382 0.009 bar^{-1}, -0.001 $^oC^{-1}$, -0.004 bar^{-1}, 30.195 ^oC and 101.896 bar, respectively. As
383 expected, the statistical parameters of the general model exhibited a worse fit (R^2_{avg} =
384 0.923 and $RMSE_{avg}$ = 0.561) than the average of the individual fits (R^2_{avg} = 0. 986;
385 $RMSE_{avg}$ = 0.198) to each survival curve obtained at each temperature and pressure for
386 *S. cerevisiae*. However, according to the R^2 and RMSE values, the proposed model
387 appropriately described the inactivation kinetics of *S. cerevisiae* with SC-CO_2+HPU as

388 a function of the temperature, pressure and time of treatment, in the practical range of
389 100-350 bar and 31-41 ºC.

390 3.3. Morphological changes in *E. coli* cells treated with SC-CO_2 and SC-CO_2+HPU.

391 In Fig. 4A, the typical rod-shaped morphology of untreated *E. coli* cells, uniformly
392 stained with toluidine blue can be observed by LM; these measured 0.67 ± 0.13 µm in
393 width and 1.19 ± 0.16 µm in length. The TEM image revealed (Fig. 4B) that the
394 intracellular organization of untreated *E. coli* cells exhibited an intact cytoplasm with a
395 uniform distribution of the inner material. The cytoplasmic content occupied the whole
396 of the intracellular space that appeared surrounded by an intact cell membrane or
397 plasmalemma and cell wall. In Fig. 4C, the intact plasmalemma and cell wall can be
398 observed in detail, with a well-defined outer membrane, peptidoglycan layer and inner
399 membrane, measuring approximately 4.5 ± 1.6 nm, 8.7 ± 1.5 nm and 4.7 ± 0.7 nm in
400 thickness, respectively.

401 The LM image of SC-CO_2-treated *E. coli* cells is shown in Fig. 4D, where little
402 stained cells were observed and the intracellular organization exhibited both an uneven
403 distribution and some aggregation of cytoplasmic content. In addition, a portion of the
404 SC-CO_2-treated *E. coli* cells, which measured 0.76 ± 0.23 µm in width and 1.40 ± 0.78
405 µm in length, had lost their typical rod-shaped morphology, although no significant
406 differences ($p>0.05$) were found compared to the dimensions of non-treated *E. coli*
407 cells. The cytoplasm content inside the SC-CO_2-treated cells observed by TEM (Figs.
408 4E and 4F) showed empty regions, which could be due to the aggregation or
409 precipitation of internal cell components, or to the removal of part of the cytoplasmic
410 content, which could be observed outside cells (Figs. 4D and 4E). The cell wall and the
411 plasmalemma of SC-CO_2-treated *E. coli* cells can be identified in some cells (Fig. 4F),
412 but modifications can be observed, compared to untreated *E. coli* cells. The

plasmalemma appeared to be disintegrated in some areas while the thickness of the outer membrane, the peptidoglycan layer and the inner membrane measured 6.2 ± 0.9 nm, 11.8 ± 1.9 nm and 3.8 ± 0.5 nm, respectively, with a significantly ($p<0.05$) thicker outer membrane and peptidoglycan layer than in the untreated *E. coli* cells. This could be due to the fact that the peptidoglycan layer was observed with a higher degree of dissolution and a loss of cohesiveness was observed in the outer membrane, as were protuberances and winding, through which the intracellular content could be extracted. This is a consequence of the amount of CO_2 accumulated in the lipid phase, which structurally and functionally disrupts the cell membrane due to a loss of integrity and order of the lipid chain, which increases the fluidity and, hence, the permeability of the membrane (Giulitti, Cinquemani, & Spilimbergo, 2011).

Garcia-Gonzalez et al. (2010) compared TEM micrographs of untreated and treated *E. coli* cells, under SC-CO_2 at 210 bar and 45 ºC 60 min, and observed that the cytoplasm of the treated cells bulged through small pores in the cell wall and seemed to have lost its coherence. Liao et al. (2010a) examined the morphology of SC-CO_2-treated *E. coli* (100 bar, 37 ºC, 75 min) by TEM and concluded that the SC-CO_2 treatment provoked morphological changes on the surfaces of treated cells. The process times used in the cited studies (Garcia-Gonzalez et al., 2010; Liao et al., 2010a) were 60 and 75 min and both attained a reduction of 7-9 log-cycles after the treatment. However, in the present study the process time applied was 5 min and only a reduction of 0.3±0.06 log-cycles was achieved. Therefore, 5 min of SC-CO_2 treatment generated the uneven internal cellular distribution; however, although the external morphology was slightly modified, no inactivation of the cells was obtained. It could be due to the fact that these slight alterations inside the cells and in the cell envelope may be reversible. As the contact between cells and CO_2 was broken, the cells probably synthesized new

biomolecules to repair damage to the cell walls and membranes so as to continue the cellular division and growth (Erkmen, & Bozoglu, 2008). Spilimbergo, Mantoan, Quaranta, & Mea (2009) observed that the initial damage of the cellular envelope is not lethal for the cell. These authors observed that SC-CO_2 treatments (100 bar, 36 ºC) of over 10 min were required to induce irreversible damage to the cells, causing their death.

The SC-CO_2+HPU treatment (Fig. 4G-I) generated more morphological changes than the SC-CO_2 treatment (Fig. 4D-F). Significant differences ($p<0.05$) were found in the dimensions of the SC-CO_2+HPU treated *E. coli* cells, 1.20 ± 0.32 µm in width and 2.51 ± 1.15 µm in length, compared to non-treated and SC-CO_2 treated *E. coli* cells. It could be due to the expansion of the cytoplasmic content after depressurization or to the accumulation of CO_2 inside the cells. In the LM image (Fig. 4G), it can be perceived that SC-CO_2+HPU-treated *E. coli* cells appeared less stained than untreated (Fig. 4A) and SC-CO_2 treated (Fig. 4D) ones. Numerous aggregates (intensively blue stained) of cytoplasmic content could be observed surrounding the SC-CO_2+HPU treated cells (Fig 4G). TEM images of SC-CO_2+HPU treated cells (Fig. 4H-I) revealed a higher aggregation and more uneven distribution of the cytoplasmic content compared to SC-CO_2 treated cells. Great proportions of empty regions were observed inside the SC-CO_2+HPU-treated cells, clearly indicating a drastic reduction in the cytoplasmic content. The outer membrane, peptidoglycan layer, inner membrane of the cell wall and plasmalemma appeared to be disintegrated and separated from the inner cell in most of the bacteria (Figs. 4H-I).

In the present study, the SC-CO_2+HPU treatment totally inactivated the population of *E. coli* (8.3 log-cycles) and generated more severe effects on the morphology of cells than the SC-CO_2 treatment. The greatest differences between the effects of both

treatments can be found in the integrity of the cell wall and plasmalemma, which were totally disrupted after the SC-CO_2+HPU treatment. This fact could expedite the loss of the *E. coli* cells' integrity, resulting in the microorganism inactivation. The inactivation effect of the SC-CO_2+HPU treatment could be related to the cavitation phenomenon generated by HPU which could damage the cell wall and membranes increasing both the rupture of the cellular envelope and the disintegration and dispersion of the intracellular content. Moreover, the agitation produced by the ultrasonic field could accelerate the solubilization rate of SC-CO_2 into the liquid and increase the mass transfer rates (Awad, Moharram, Shaltout, Asker, & Youssef, 2012), drastically affecting the cell membrane and facilitating the inactivation mechanisms associated with SC-CO_2 treatments.

3.4. Morphological changes in *S. cerevisiae* cells treated with SC-CO_2 and SC-CO_2+HPU

Fig. 5A shows the typical ellipsoidal morphology of untreated *S. cerevisiae* cells observed by LM, which typically measured 3.11 ± 0.40 µm at the large diameter and 2.63 ± 0.23 µm at the small one. The cells appeared homogeneously stained and the budding process could be noted in some of them. TEM images (Figs 5B, 5C) depict a compact and homogeneous distribution of the cytoplasm, in which the following could be distinguished: a well-defined nucleus, a nuclear membrane, vacuoles, the intact plasmalemma, the cell wall with an electron-transparent internal layer, consisting of β-1, 3-glucan and chitin, the thicknesses of which were about 84.1 ± 16.7 nm and an electron-dense and osmiophilic outer layer, mainly corresponding to glycosylated mannoproteins, of about 40.7 ± 11.3 nm. The plasmalemma or cell membrane also appeared to be well-preserved and close to the cell wall.

The LM image of SC-CO_2-treated *S. cerevisiae* cells allowed less intensely stained cells than untreated yeasts to be observed in Fig. 5D, which indicates a lower intracellular content inside the cells. Moreover, some areas more intensely stained outside the cells, revealing the removal of their cytoplasmic content. In general, no significant differences ($p>0.05$) in size were found between SC-CO_2-treated cells, which measured 3.33 ± 0.50 µm at the large diameter and 2.69 ± 0.48 µm at the small one, and untreated cells. Inside the cells, a loss in cytoplasm integrity could be observed, as could the disappearance of the nucleus, the desegregation of cytoplasmic organelles and the aggregation of some cytoplasmic substances (AC, Fig. 5E). An examination of the treated cells revealed that the cell wall still contained layers (Fig. 5F), an internal layer of about 101.8 ± 19.5 nm in thickness and an outer layer of about 54.7 ± 11.5 nm, both significantly ($p<0.05$) thicker than in the non-treated *S. cerevisiae* cells, which could be due to the accumulation of CO_2 in the cell membrane. The inner layer could be observed as more densely stained and the outer layer thicker than those of untreated cells (Fig. 5F). TEM observations confirmed that in some cells, the SC-CO_2 treatment provoked the degradation and dissolution of some constituents of cell walls, which could be related to the CO_2 lipophilic solvent characteristics (Giulitti et al., 2011). This fact could increase the permeability and fluidity of cell wall and cell membrane. In many locations, plasmalemma could not be visualized and some cells contained abnormal bud scars (Fig. 5F).

Garcia-Gonzalez et al. (2010) investigated the effect of SC-CO_2 (210 bar, 45 ºC for 60 min) on the morphology of *S. cerevisiae* and concluded that, despite the membrane not being disrupted, its permeabilization could ease the penetration of CO_2 into the cell and the pH drop could induce a denaturation of some key enzymes. Li, Deng, Chen, & Liao (2012) explored the differences between untreated and treated *S. cerevisiae* cells at

512 100 bar and 35 ºC for different process times: 30, 75 and 120 min, by SEM and TEM,
513 and revealed that the intracellular content in the treated cells gradually weakened as the
514 treatment time increased; they also observed the reduction of the cytoplasm density and
515 the extraction of cytoplasmic content, in spite of the fact that the cell walls remained
516 intact. In the present work, after only 5 min of SC-CO_2 treatment, the CO_2 succeeded in
517 penetrating the cells, generating minor irregularities which were not sufficient to
518 observe an important microbial reduction of *S. cerevisiae* (0.2 log-cycles). It is possible
519 that *S. cerevisiae* cells synthesize new biomolecules after 5 min of treatment to repair
520 the damaged cell walls and membranes so as to continue cellular division and growth
521 (Erkmen, & Bozoglu, 2008). Thus, longer process times may be required to inactivate
522 enough key enzymes and to affect the cellular envelope, which would allow a
523 significant reduction of surviving *S. cerevisiae* cells to be obtained.

524 Significant differences ($p<0.05$) were found in the dimensions of the SC-
525 CO_2+HPU- treated *S. cerevisiae* cells, 4.15 ± 0.77 µm in width and 5.76 ± 0.77 µm in
526 length, compared to non-treated and SC-CO_2- treated *S. cerevisiae* cells. The greater
527 size observed in SC-CO_2+HPU-treated cells could be due to the larger expansion of the
528 cytoplasmic content after depressurization or to the accumulation of CO_2 inside the
529 cells. LM images (Fig. 5G) showed that the SC-CO_2+HPU treatment provoked a higher
530 degree of cellular degradation, compared to the SC-CO_2 treatment. In addition to the
531 fact that the SC-CO_2+HPU- treated cells exhibited a lower degree of staining (Fig. 5G),
532 it was possible to observe a greater amount of intracellular content extracted from the
533 cells. The TEM images revealed lemon-shaped deformed cells (Fig. 5H), with
534 punctured or broken walls, disrupted organelles, cytoplasm retracted from the cell wall
535 and a large proportion of empty regions. Fig. 5I shows that the cell walls had partially
536 lost their layered structure. The inner layer appeared to be more densely stained due to

537 the possible diffusion of intracellular content through it, which hinders a clear
538 differentiation between the outer and the inner layer. The inner and the outer layer
539 measured 165.7 ± 32.3 nm and 96.8 ± 15.7 nm in thickness, respectively, both being
540 significantly ($p<0.05$) thicker than in the non-treated and SC-CO_2 treated *S. cerevisiae*
541 cells. The plasmalemma appeared to be degraded and was not visible. Moreover, it can
542 be noted that the TEM images revealed that the SC-CO_2+HPU treatment caused an
543 important degradation of the content in the majority of cells, with the disappearance of
544 the nucleus, the disruption and degradation of cytoplasmic organelles, and the creation
545 of vesicles on the outer side of the plasmalemma.

546 The SC-CO_2+HPU treatment produced the total inactivation of *S. cerevisiae* after
547 5 min of treatment, compared to the 0.2 log-cycles attained after 5 min of the SC-CO_2
548 treatment. By observing the TEM images of both treatments (Figures 5E, 5H), it can be
549 observed that the greatest difference appeared to be between the disrupted cell envelope
550 (cell wall) and the plasmalemma of the SC-CO_2+HPU-treated cells and the almost intact
551 ones of the SC-CO_2-treated cells. Therefore, the faster microbial inactivation achieved
552 by the SC-CO_2+HPU treatment compared to that of SC-CO_2, could be due to the
553 cavitation phenomenon generated by HPU which could cause cracked or damaged cell
554 walls. This enhances the penetration of SC-CO_2 inside the cells, changing the cellular
555 equilibrium and facilitating the extraction of intracellular compounds, thus accelerating
556 the death of the microbial cells.

557 3.5. Stability of treated samples during refrigerated storage

558 The stability of the samples treated with SC-CO_2+HPU was analyzed while they
559 were stored for 6 weeks at 4 ºC. The regrowth or survival of the SC-CO_2+HPU- treated
560 *E. coli* and *S. cerevisiae* cells was not observed during the 6-weeks storage period.
561 These results could suggest that the treated cells were not capable of recovering during

562 their storage on LB or YPD Broth. Therefore, the SC-CO_2+HPU treatment generated
563 irreversible damage to the cells, as observed in the microstructural analysis, preventing
564 a possible synthesis of new biomolecules which would repair the damage to the cell
565 walls and membranes and preventing the cellular division and growth.

566 Using only SC-CO_2, other studies have observed a growth in the microbial
567 population during a post-treatment storage period (Kincal, Hill, Balaban, Portier, Wei,
568 & Marshall, 2005; Fabroni, Amenta, Timpanaro, & Rapisarda, 2010) although at time 0
569 (immediately after the treatment) no microorganisms were detected.

570 Liao, Zhang, Hu, & Liao (2010b) investigated the inactivation and the possible
571 regrowth of natural microorganisms in apple juice after a SC-CO_2 treatment (200 bar,
572 52-62 ºC, 30 min). The population of aerobic bacteria in apple juice, subjected to SC-
573 CO_2, exhibited no increase during storage for 35 days at 2 °C; however, the population
574 of yeasts and moulds slightly increased after 14 storage days. In the present study, using
575 SC-CO_2+HPU, shorter process times and lower temperatures, no microbial growth was
576 detected during a longer storage period. Therefore, the application of HPU during the
577 SC-CO_2 treatment increased the damage caused to the microorganisms, thus avoiding
578 microbial recovery.

579 **4. CONCLUSIONS**

580 Shorter process times were required to achieve the total inactivation of *S. cerevisiae*
581 than of *E. coli*, despite the fact that the yeast is known to have a greater resistance to
582 SC-CO_2. This could be due to the fact that the *S. cerevisiae* cells are bigger and, as such,
583 the cavitation bubbles associated with HPU have a more marked effect on them.

584 The microstructural study carried out in the present work revealed that there was a
585 direct relationship between cellular modification/damage and inactivation provoked by

586 the SC-CO_2 and SC-CO_2+HPU treatments on *E. coli* and *S. cerevisiae* cells. Despite the
587 small changes observed in cell morphology after 5 min of the SC-CO_2 treatment, the
588 treatment was not lethal against either *E. coli* or *S. cerevisiae*. However, 5 min of
589 the SC-CO_2+HPU treatment totally inactivated the population of both microorganisms.
590 After the SC-CO_2+HPU treatment, cell wall and cell membrane were totally disrupted,
591 thus easing the disintegration of the cytoplasm and the inactivation of cells. The damage
592 caused by the SC-CO_2+HPU treatment was serious enough to prevent a possible
593 regrowth of cells during post-treatment storage.

594 SC-CO_2+HPU is a non-thermal preservation technology that could represent an
595 alternative means to thermal processing to extend the shelf life of foods using mild
596 process conditions.

597

598 **Acknowledgments**

599 The authors acknowledge the financial support from project CSD2007-00016
600 (CONSOLIDER-INGENIO 2010, Spanish Ministry of Science and Innovation) and
601 from project PROMETEO/2010/062; Generalitat Valenciana. We thank Dr. Emilia
602 Matallana and Dr. Paula Alepuz for the generous gift of *S. cerevisiae* T73 and *E. coli*
603 DH1 strains, respectively.

604

605 **References**

606 Awad, T.S., Moharram, H.A., Shaltout, O.E., Asker, D., & Youssef, M.M. (2012).
607 Applications of ultrasound in analysis, processing and quality control of food: A review.
608 *Food Research International, 48,* 410-427.

609 Benedito, J., Martínez-Pastor, M. T., Mulet, A., Ortuño, C., & Peña, R. (2011).
610 Procedure of microorganisms inactivation by combination of supercritical fluids and
611 ultrasound. Spain. Patent No. P201131099.

612 Corradini, M.G., & Peleg, M., 2012. The kinetics of microbial inactivation by carbon
613 dioxide under high pressure, in M.O. Balaban & G. Ferrentino (Eds.), *Dense phase*
614 *carbon dioxide: food and pharmaceutical applications* (pp. 135-155). Iowa, USA:
615 Blackwell Publishing Professional.

616 Erkmen, O. (2003). Mathematical modeling of *Saccharomyces cerevisiae*
617 inactivation under high-pressure carbon dioxide. *Nahrung-Food, 47*, 176-180.

618 Erkmen, O. (2012). Effects of Dense Phase Carbon Dioxide on Vegetative Cells, in
619 M.O. Balaban & G. Ferrentino (Eds.), *Dense phase carbon dioxide: food and*
620 *pharmaceutical applications* (pp. 67-97). Iowa, USA: Blackwell Publishing
621 Professional.

622 Erkmen, O., & Bozoglu, T.F. (2008). Food Microbiology I: *Microorganisms in*
623 *Foods, Microbial Growth, Foodborne Diseases and Detection of Microorganisms and*
624 *Their Toxins*. Ankara: Ilke Publishing Company.

625 Fabroni, S., Amenta, M., Timpanaro, N., & Rapisarda, P. (2010). Supercritical
626 carbon dioxide-treated blood orange juice as a new product in the fresh fruit juice
627 market. *Innovative Food Science and Emerging Technologies, 11*, 477-484.

628 Ferrentino, G., Balaban, M., Ferrari, G., & Poletto, M. (2010). Food treatment with
629 high pressure carbon dioxide: *Saccharomyces cerevisiae* inactivation kinetics expressed
630 as a function of CO_2 solubility. *Journal of Supercritical Fluids, 52*, 151-160.

631 Garcia-Gonzalez, L., Geeraerd, A.H., Spilimbergo, S., Elst, K., Van Ginneken, L.,
632 Debevere, J., Van Impe, J.F., & Devlieghere, F. (2007). High pressure carbon dioxide

633 inactivation of microorganisms in foods: the past, the present and the future.
634 *International Journal of Food Microbiology, 117*, 1-28.

635 Garcia-Gonzalez, L., Geeraerd, A. H., Mast, J., Briers, Y., Elst, K., Van Ginneken,
636 L., Van Impe, J.F., & Devlieghere, F. (2010). Membrane permeabilization and cellular
637 death of *Escherichia coli*, *Listeria monocytogenes* and *Saccharomyces cerevisiae* as
638 induced by high pressure carbon dioxide treatment. *Food Microbiology, 27*, 541-549.

639 Giulitti, S., Cinquemani, C., & Spilimbergo, S. (2011). High Pressure Gases: Role of
640 Dynamic Intracellular pH in Pasteurization. *Biotechnology & Bioengineering, 108*,
641 1211-1214.

642 Kincal, D., Hill, W.S., Balaban, M.O., Portier, K.M., Wei, C.I., & Marshall, M.R.
643 (2005). A continuous high pressure carbon dioxide system for microbial reduction in
644 orange juice. *Journal of Food Science, 70*, 249-254.

645 Kumar, S., Thippareddi, H., Subbiah, J., Zivanovic, S., Davinson, P.M., & Harte, F.
646 (2009). Inactivation of *Escherichia coli* K-12 in apple juice using combination of high
647 pressure homogenization and chitosan. *Journal of Food Science, 74*, 8-14.

648 Laun, P., Pichova, A., Madeo, F., Fuchs, J., Ellinger, A., Kohlwein, S., Dawes, I.,
649 Fröhlich, K. U., & Breitenbach, M. (2001). Aged mother cells of *Saccharomyces*
650 *cerevisiae* show markers of oxidative stress and apoptosis. *Molecular microbiology, 39*,
651 1166-1173.

652 Lee, H., Zhou, B., Liang, W., Feng, H., & Martin, S.E. (2009). Inactivation of
653 *Escherichia coli* cells with sonication, manosonication, thermosonication, and
654 manothermosonication: Microbial responses and kinetics modeling. *Journal of Food*
655 *Engineering, 93*, 354-364.

Li, H., Deng, L., Chen, Y., & Liao, X. (2012). Inactivation, morphology, interior structure and enzymatic activity of high pressure CO_2 treated *S. cerevisiae*. *Innovative Food Science and Emerging Technologies, 14*, 99-106.

Liao, H., Hu, X., Liao, X., Chen, F., & Wu, J. (2006). Inactivation of *Escherichia coli* inoculated into cloudy apple juice exposed to dense phase carbon dioxide. *International Journal of Food Microbiology, 118*, 126-131.

Liao, H., Zhang, F., Liao, X., Hu, X., Chen, Y., & Deng, L. (2010a). Analysis of *Escherichia coli* cell damage induced by HPCD using microscopies and fluorescent staining. *International Journal of Food Microbiology, 144*, 169-176.

Liao, H., Zhang, L., Hu, X. & Liao, X. (2010b). Effect of high pressure CO_2 and mild heat processing on natural microorganisms in apple juice. *International Journal of Food Microbiology, 137,* 81-87.

Nelson, D.E., & Young, K.D. (2000). Penicillin binding protein 5 affects cell diameter, contour, and morphology of *Escherichia coli* (Statistical Data Included). *Journal of Bacteriology, 182,* 1714-1719.

Ortuño, C., Martínez-Pastor, M.T., Mulet, A., & Benedito, J. (2012a). An ultrasound-enhanced system for microbial inactivation using supercritical carbon dioxide. *Innovative Food Science and Emerging Technologies, 15*, 31-37.

Ortuño, C., Martínez-Pastor, M.T., Mulet, A., & Benedito, J. (2012b). Supercritical carbon dioxide inactivation of *Escherichia coli* and *Saccharomyces cerevisiae* in different growth stages. *Journal of Supercritical Fluids, 63*, 8-15.

Ortuño, C., Martínez-Pastor, M. T., Mulet, A., & Benedito, J. (2013). Application of high power ultrasound in the supercritical carbon dioxide inactivation of *Saccharomyces cerevisiae*. *Food Research International, 51,* 474-481.

680 Peleg, M. 2006. *Advanced Quantitative Microbiology for Foods and Biosystems*.
681 Florida, EE.UU, CRC Boca Raton.

682 Rawson, A., Patras, A., Tiwari, B.K., Noci, F., Koutchma, T., & Brunton, N. (2011).
683 Effect of thermal and non thermal processing technologies on the bioactive content of
684 exotic fruits and their products: Review of recent advances. *Food Research*
685 *International 44,* 1875-1887.

686 Schemper, M., 2003. Predictive accuracy and explained variation. Statistics in
687 Medicine 22, 2299-2308.

688 Shimoda, M., Yamamoto, Y., Cocunubo-Castellanos, J., Tonoike, H., Kawano, T.,
689 Ishikawa, H., & Osajima, Y. (1998). Antimicrobial effects of pressured carbon dioxide
690 in a continuous flow system. *Journal of Food Science, 63*, 709-712.

691 Spilimbergo, S., Mantoan, D., & Dalser, A. (2007). Supercritical gases
692 pasterurization of apple juice. *Journal of Supercritical Fluids, 40*, 485-489.

693 Spilimbergo, S., Mantoan, D., Quaranta, A., & Mea, G. D. (2009). Real-time
694 monitoring of cell membrane modification during supercritical CO_2 pasteurization.
695 *Journal of Supercritical Fluids, 48*, 93-97.

696 Tahiri, I., Makhlouf, J., Paquin, P., & Fliss, I. (2006). Inactivation of food spoilage
697 bacteria and *Escherichia coli* O157:H7 in phosphate buffer and orange juice using
698 dynamic high pressure. *Food Research International, 39*, 98-105.

699

700

Figure Captions

Figure 1. Supercritical CO_2 treatment system. 1-CO_2 tank; 2-N_2 tank; 3-Chiller reservoir; 4-Pump; 5-Temperature controlled bath; 6-Treatment vessel; 7-Temperature Sensor; 8-Transducer; 9-Insulation joint; 10-Ceramics; 11-Power Generation Unit; 12-Sample extraction; V-Valve; P-Manometer.

Figure 2. Experimental data (discrete points) and modeling (continuous line) of the inactivation kinetics of *E. coli* in apple juice treated by SC-CO_2 and HPU at different temperatures (A, 225 bar) and pressures (B, 36 ºC). **P. Type A:** General Peleg Type A model.

Figure 3. Experimental data (discrete points) and modeling (continuous line) of the inactivation kinetics of *S. cerevisiae* in apple juice treated by SC-CO_2+HPU at different temperatures (A, 225 bar) and pressures (B, 36 ºC). **M:** modified Weibull model.

Figure 4. LM (A, D, G) and TEM (B, C, E, F, H, and I) micrographs by semithin and ultrathin sectioning of *E. coli*. Images A-C represent untreated cells; images D-F show cells treated with SC-CO_2 at 350 bar, 36 ºC for 5 min; images G-I show cells treated with SC-CO_2+HPU at 350 bar, 36 ºC, 40 W for 5 min. OM: cell wall-outer membrane; PL: cell wall-peptidoglycan layer; IM: cell wall-inner membrane; ER: empty regions; CC: cytoplasmic content.

Figure 5. LM (A, D, G) and TEM (B, C, E, F, H, and I) micrographs by semithin and ultrathin sectioning of *S. cerevisiae*. Images A-C represent untreated cells; images D-F show cells treated with SC-CO_2 at 350 bar, 36 ºC for 5 min; images G-I show cells treated with SC-CO_2+HPU at 350 bar, 36 ºC, 40 W for 5 min. BP: budding process; N: nucleus; NM: nuclear membrane; V: vacuoles; PM: plasmalemma; IL: cell wall-internal layer; OL: cell wall-outer layer; CC: cytoplasmic content; ER: empty regions; CW: cell wall; ACC: aggregation cytoplasmic content; ABS: abnormal bud scars; CR: cytoplasm retracted; VE: vesicles.

Figure 1

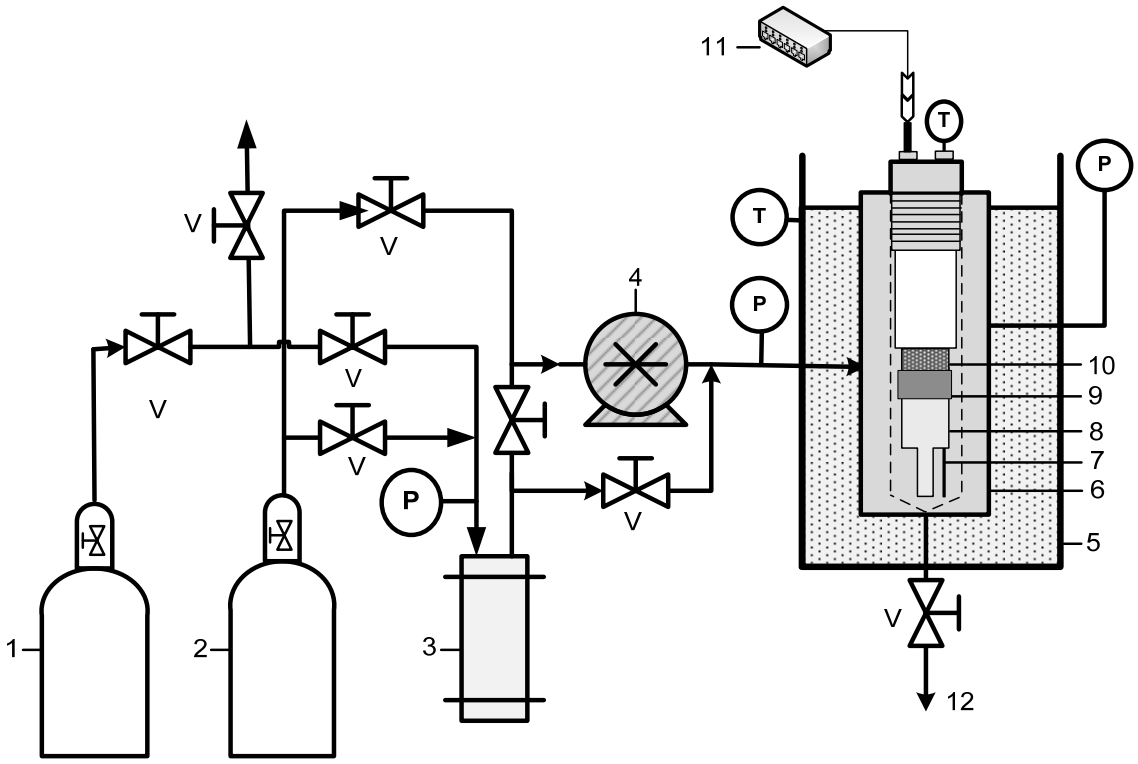

Figure 2

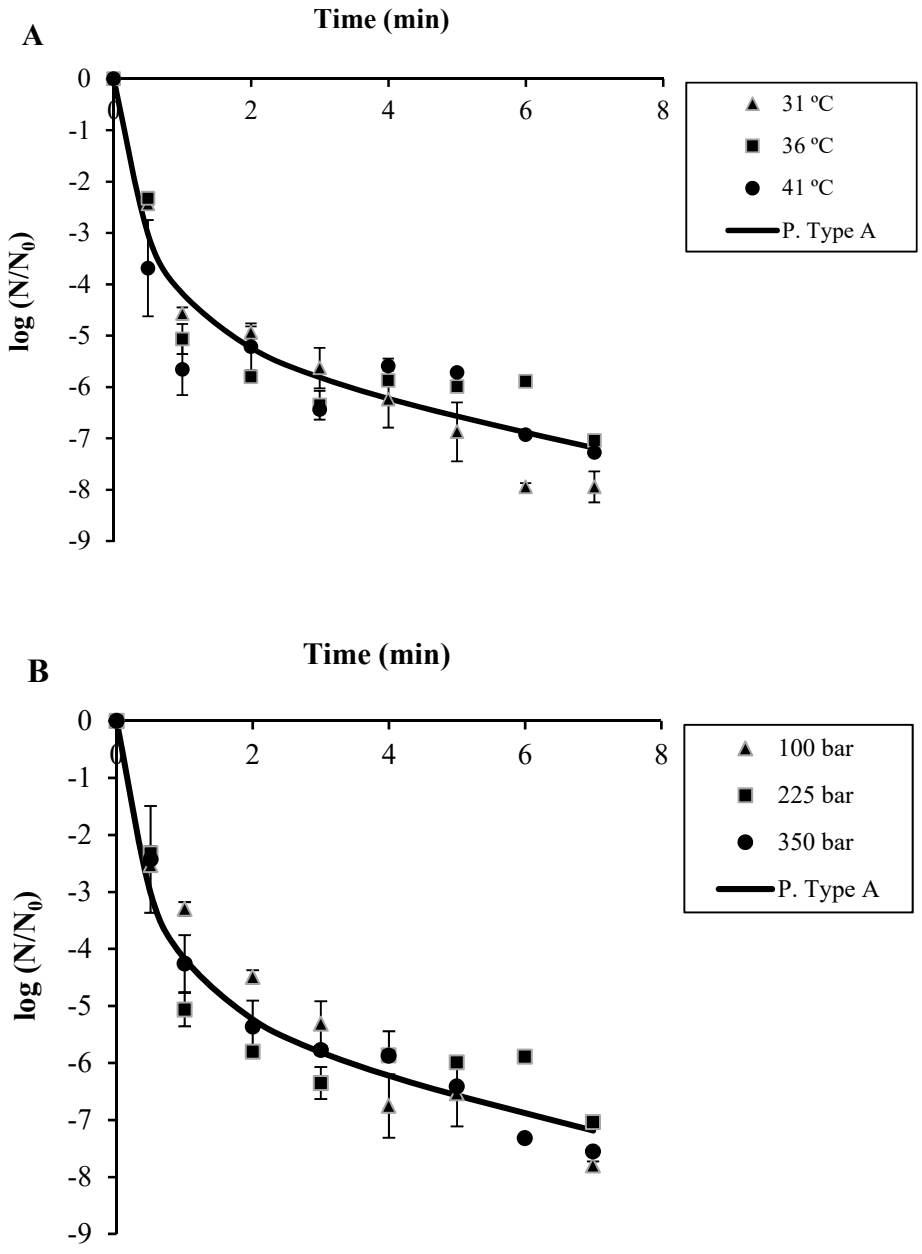
A
Time (min)
log (N/N0)
0
-1
-2
-3
-4
-5
-6
-7
-8
-9
0
2
4
6
8
31 ºC
36 ºC
41 ºC
P. Type A
B
Time (min)
log (N/N0)
100 bar
225 bar
350 bar
P. Type A

Figure 3

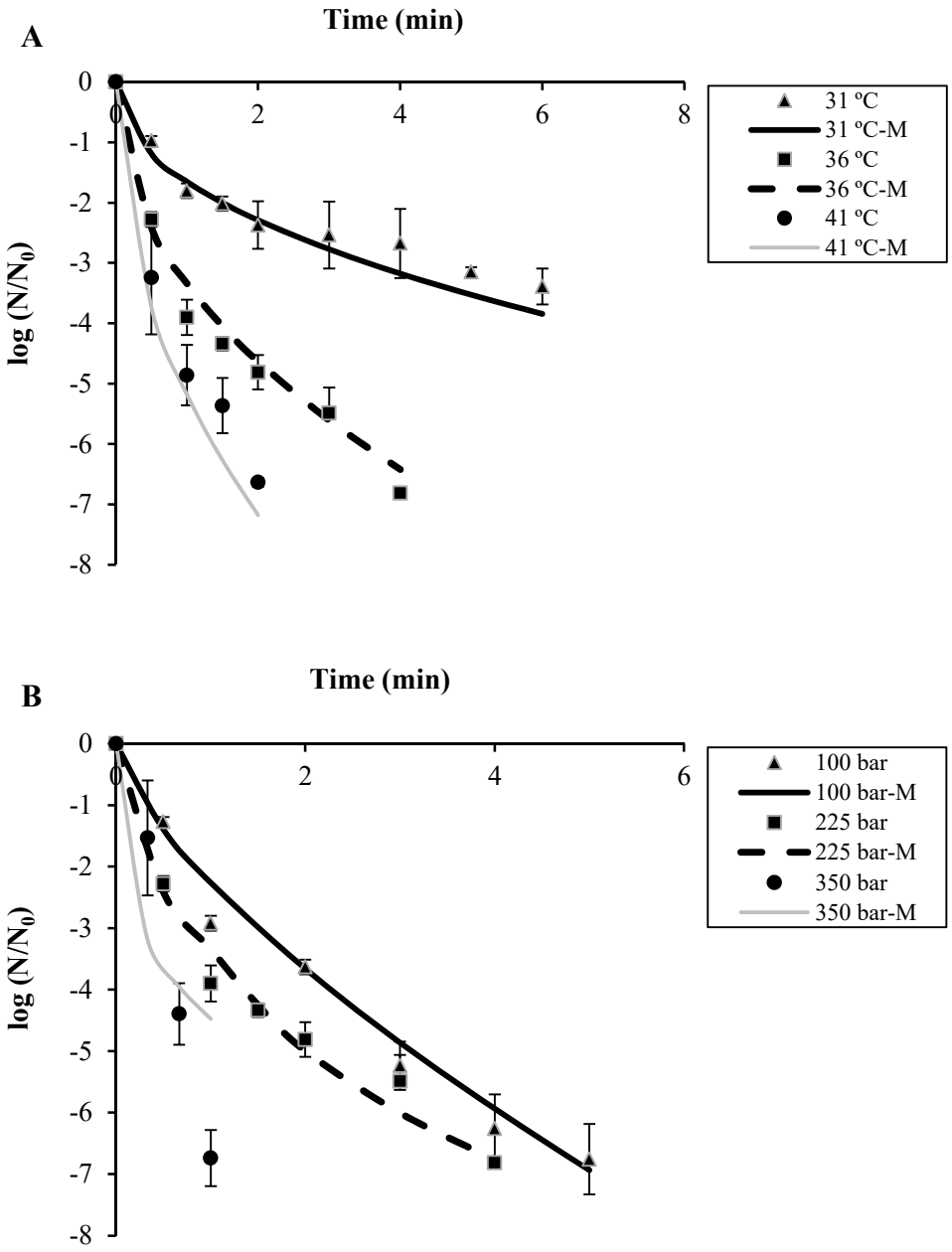
A
Time (min)
log (N/N0)
0
-1
-2
-3
-4
-5
-6
-7
-8
0
2
4
6
8
31 ºC
31 ºC-M
36 ºC
36 ºC-M
41 ºC
41 ºC-M
B
Time (min)
log (N/N0)
0
-1
-2
-3
-4
-5
-6
-7
-8
0
2
4
6
100 bar
100 bar-M
225 bar
225 bar-M
350 bar
350 bar-M

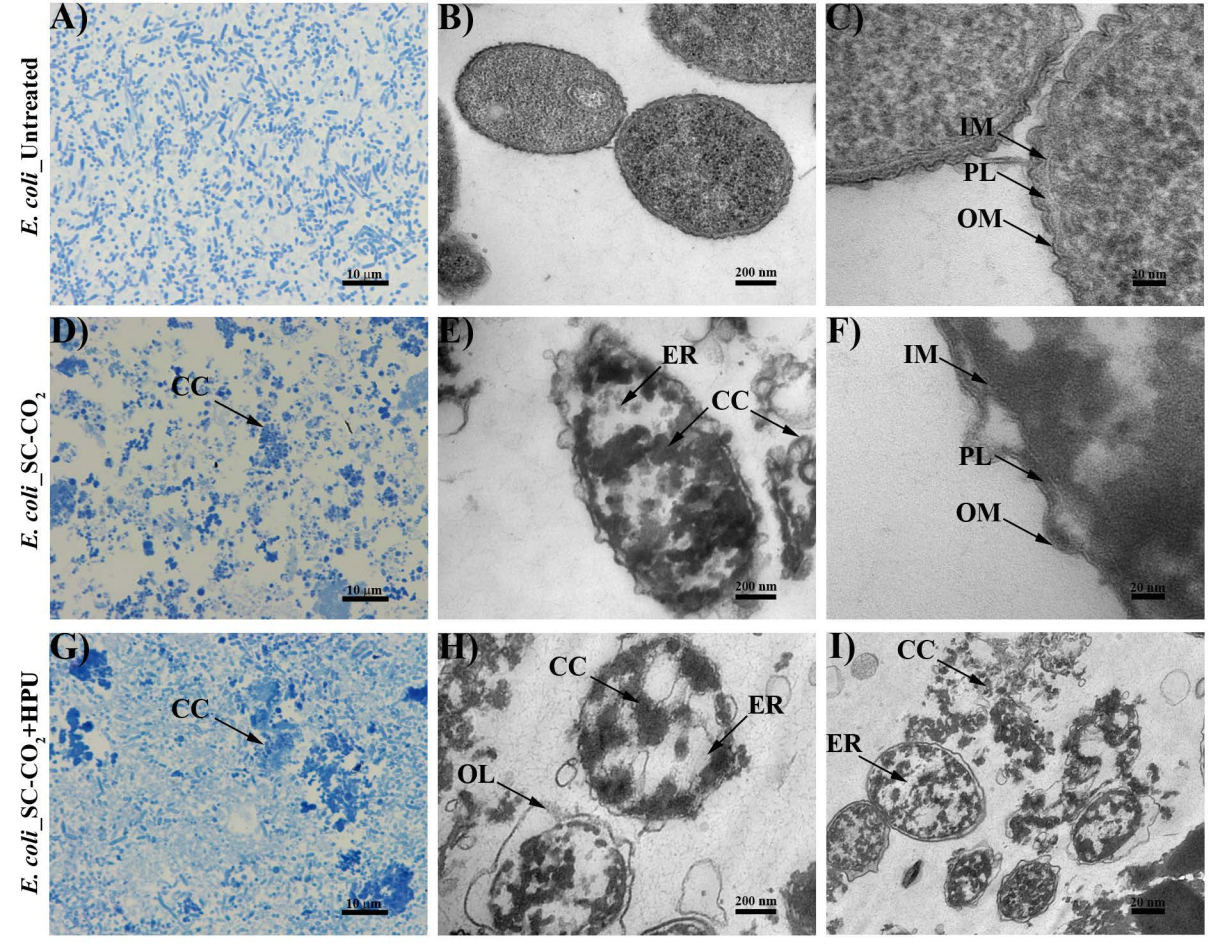
A)
B)
C)
D)
E)
F)
G)
H)
I)
E. coli_Untreated
E. coli_SC-CO2
E. coli_SC-CO2+HPU
10 µm
200 nm
20 nm
IM
PL
OM
CC
ER
OL

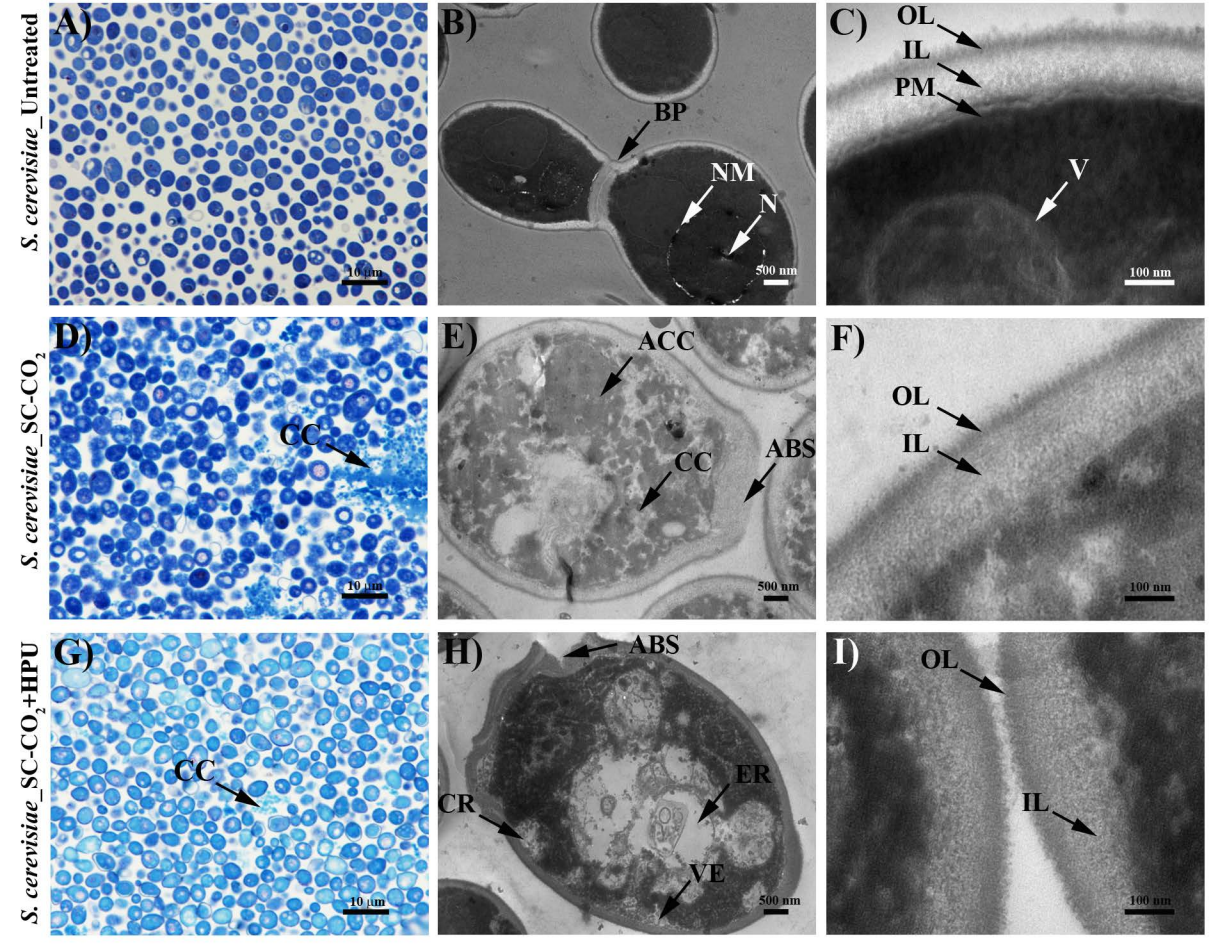
S. cerevisiae_Untreated
S. cerevisiae_SC-CO2
S. cerevisiae_SC-CO2+HPU
A)
B)
C)
D)
E)
F)
G)
H)
I)
BP
NM
N
OL
IL
PM
V
CC
ACC
ABS
CR
ER
VE
10 µm
500 nm
100 nm

Table 1. Models used to fit the microbial inactivation kinetics by SC-CO_2+HPU.

Modelling of the microbial inactivation kinetics			
Model	**Equation**	**Parameters**	**Reference**
Weibull	$\log_{10}\left(\frac{N}{N_0}\right) = -b\ t^n$	b, n	Corradini & Peleg, 2012
Biphasic	$\log_{10}\left(\frac{N}{N_0}\right) = \log_{10}\left[(1-f)\,10^{\frac{-t}{Dsens}} + f\,10^{\frac{-t}{Dres}}\right]$	f, D_{sens}, D_{res}	Lee et al., 2009
Peleg Type A	$\log_{10}\left(\frac{N}{N_0}\right) = -\frac{a_1 t}{(1+a_2 t)(a_3 - t)}$	a_1,a_2 ,a_3	Peleg, 2006
Peleg Type B	$\log_{10}\left(\frac{N}{N_0}\right) = -\frac{b_1 t^r}{b_2 + t^r}$	b_1, b_2, r	Peleg, 2006

N_0: the initial number of microorganisms at time 0; N: the corresponding number after a time t.
b: non-linear rate parameter; n is the shape factor.
(1-f) and f: the fraction of treatment-sensitive and treatment-resistant population, respectively; D_{sens} and D_{res} are the decimal reduction times of the two populations (min)
a_1, a_2, a_3, b_1, b_2, r: model parameters

Table 2. Statistical parameters for the fit of the kinetic models to the inactivation data of *E. coli* and *S. cerevisiae* in apple juice treated by SC-CO_2 and HPU at three temperatures (31, 36 and 41 ºC, at constant P = 225 bar) and three pressures (100, 225 and 350 bar, at constant T = 36 ºC).

		Escherichia coli				***Saccharomyces cerevisiae***			
Treatment conditions	**Statistics**	**W**	**Bi**	**A**	**B**	**W**	**Bi**	**A**	**B**
225 bar 31 ºC	R^2	0.977	0.993	0.980	0.973	0.977	0.993	0.985	0.973
	RMSE	0.347	0.179	0.303	0.347	0.142	0.071	0.106	0.142
225 bar 36 ºC	R^2	0.887	0.971	0.933	0.868	0.985	0.995	0.973	0.981
	RMSE	0.674	0.313	0.482	0.674	0.232	0.114	0.277	0.230
225 bar 41 ºC	R^2	0.925	0.609	0.926	0.913	0.992	0.992	0.983	0.988
	RMSE	0.530	1.124	0.489	0.529	0.175	0.141	0.211	0.175
100 bar 36 ºC	R^2	0.989	0.866	0.982	0.987	0.985	0.984	0.982	0.981
	RMSE	0.236	0.745	0.270	0.233	0.264	0.239	0.255	0.264
350 bar 36 ºC	R^2	0.976	0.935	0.984	0.977	0.993	0.856	0.977	0.999
	RMSE	0.335	0.507	0.250	0.305	0.177	0.568	0.226	0.001
	R^2_{avg}	0.951	0.860	0.961	0.944	0.986	0.964	0.980	0.985
	$RMSE_{avg}$	0.425	0.591	0.386	0.446	0.198	0.141	0.212	0.203

W, Bi, A, B: Weibull, Biphasic, Peleg Type A and Peleg Type B model, respectively.